

**UPDATED PERSPECTIVE ON CHEMCAM DATA THROUGH CLUSTERING.** O. Gasnault<sup>1</sup>, O. Forni<sup>1</sup>, N Mangold<sup>2</sup>, R. Wiens<sup>3</sup>, P.-Y. Meslin<sup>1</sup>, J. Lasue<sup>1</sup>, P. Pinet<sup>1</sup>, S. Maurice<sup>1</sup>, E. Lewin<sup>4</sup>, R. Anderson<sup>5</sup>, B. Clark<sup>6</sup>, N. Melikechi<sup>7</sup>, H. Newsom<sup>8</sup>, V. Sautter<sup>9</sup>, and J. Blank<sup>10</sup>, <sup>1</sup>IRAP (Univ. Toulouse, France - ogasnault@irap.omp.eu), <sup>2</sup>LPG-Nantes, France, <sup>3</sup>LANL, Los Alamos, US, <sup>4</sup>ISTerre, Grenoble, France, <sup>5</sup>USGS, Flagstaff, USA, <sup>6</sup>PSI, Tucson, USA, <sup>7</sup>DSU, Dover, USA, <sup>8</sup>UNM, Albuquerque, USA, <sup>9</sup>IMPMC, Paris, France, <sup>10</sup>BAERI, Sonoma, USA.

**Introduction:** Curiosity encountered diverse rocks by their textures and compositions, along its traverse inside Gale Crater (Mars), including fluvio-lacustrine deposits [1], conglomerates supporting multiple sources for the sediments [2], and more recently evidences for chemical weathering [3].

Here we update the clustering analysis of ChemCam data [4, 5] in support of a more comprehensive classification of Curiosity targets [6].

ChemCam uses Laser-Induced Breakdown Spectroscopy (LIBS) to sample remotely the elemental composition of targets up to a few meters. ChemCam is sensitive to most major elements and some minor/trace elements [7, 8]. The submillimeter scale of the sampling gives access to the composition of crystals, grains, sediments, and cements.

We define 6 groups of relative uniform composition and distinct from each other, with observations up to Sol 586. We also project the most recent data (Sols 600-801) into these 6 groups to demonstrate the ability to classify new targets based on their chemistry.

**Method:** The approach is based on a hierarchical divisive clustering of scores produced by an Independent Component Analysis (ICA) of the spectra, which are normalized to their total intensity. The spectra are averages of 25 laser shots or more (the first 5 of each burst are excluded because of dust). The quantitative abundances are given by Partial Least Square processing (PLS1) [9]. The following 9 chemical elements are included in the analysis (Si, Ti, Al, Fe, Mg, Ca, Na, K, and H). Outliers characterized by high abundances in other elements are generally processed separately.

**Summary of results up to Sol 600:** This reference dataset includes 3358 measurements. To first order, the analysis distinguishes more mafic from more felsic compositions (Fig. 1), with a clear enrichment in Mg, Fe, Ti on one side and in Si, Al, Na on the other side, which is a characteristic of this landing site [10].

Among all the ChemCam measurement points, 84% show a “classical” martian mafic composition, which was found all along the traverse in both rocks and soils (the latter being characterized by a higher H signal, from a spectrum point of view, e.g. Sandy\_Dam on Sol 544). Most of these rocks were found in the Sheepbed unit (e.g. CumberlandNew\_RP, Sol 277), but similar compositions are found in all stratigraphic units and in float rocks. This group is

characterized by relatively high abundances of Fe and Ti, typically FeO<sub>T</sub> abundances between 17.1 and 19.6 wt. %, and TiO<sub>2</sub> abundances between 0.9 and 1.3 wt. %. This is also the only group showing a strong anti-correlation between Fe and Mg, and some between Fe and H. This is a large group and these trends may have various causes (orthopyroxene solid solution, mixing with iron oxides, such as magnetite and hematite, or alteration in these layers).

Calcium-sulfate veins and nodules identified by ChemCam in the Sheepbed unit (Sols 125-300) define a small but well-defined group in the mafic branch (denoted by a mixing line between mafic and calcium-sulfate end-members, which results from traces of the host rocks or variations in the vein compositions [11]). This group has the highest calcium abundances, typically between 29.3 and 51.4 wt. % CaO (e.g. Tukarak, Sol 165).

While we found a few felsic samples everywhere along the traverse, there were very few in the Sheepbed unit, and we found most of them just after landing (Bradbury area), during the traverse to Darwin waypoint (Sols 350-400), and around the Dingo Gap bifurcation (Sols 500-550). This group also can be subdivided with a group rather enriched in Ca, suggesting plagioclase minerals, while the remaining points are enriched in K, suggesting K-feldspars.

These intermediate-Ca materials (pebbles and float rocks, median abundance at 5.9 wt. % CaO) were found mostly after Sol 300 and could correspond to white feldspar crystals with Ca-rich cores [12] for the igneous materials (e.g. Harrison and Sparkle, Sol 514).

The K-rich materials were mainly found in bedrocks and float rocks between Shaler and Darwin areas (around Sols 300-400, e.g. Angmaat, Sol 337, with up to 4.8 wt. % K<sub>2</sub>O). Potassium is indeed quite discriminant between the 6 groups. This K-rich group in the felsic branch could correspond to compositions like alkali feldspar for the igneous materials [12]. Some of that material could be incorporated in small proportions to sedimentary rocks, which would explain higher K contents than expected in some observations [13, 14]. Another example is given by 4 of the 5 points measured on Chakonipau (a flat-lying, light-toned rock, just exposed at the surface in a pebbly soil, Sol 338) that are rich in Si (75 wt. % SiO<sub>2</sub>), Al (15 wt. % Al<sub>2</sub>O<sub>3</sub>), Na (3.9 wt. % Na<sub>2</sub>O), and K (4.0 wt. % K<sub>2</sub>O).

**New data since Sol 600:** We computed the barycenters of the 6 groups defined so far as the mean composition weighted by the silhouette parameter [15], which quantifies the clustering quality for each target. It is then possible for each of the 1902 new measurements to compute (in the ICA compositional space) the distance to the center of the groups and to compare it with the typical distances of well classified targets.

With only 3 exceptions (1 point on Kittery, Quechee\_Gorge, and Crystal\_Spring), all the targets post Sol 600 can fall in the pre-defined groups. Although a new clustering analysis suggests slightly different groupings, in which Fe vs. Ti on one side and K vs. Na on the other side could play more important roles in the subdivisions of the main branches. Less Ca-rich points were measured on rocks, even though the Ca/Si ratio tends to increase in aeolian deposits [16]. However, observations at the most recent rover waypoint: Pahrump Hills (since Sol 758), reveal many diagenetic features, including Ca-rich veins, which will change again the definition of that group along the traverse [17].

**Conclusions:** The initial clustering seems robust as the vast majority of new measurements relates to one of its groups. Even if this suggests some common sources with materials encountered before by the rover, we also see some changes since Curiosity arrived at the base of Aeolis Mons (Mount Sharp) in the target chemical compositions [18]. Consequently, it may eventually become necessary to define a new group or

a subdivision in a pre-existing group. A statistical test can be developed to decide if the clustering must be revised by checking occasionally the consistency of the groups, for example through silhouette calculations or standard deviation profiles of target distances to the cluster centers. In future steps, the clustering can be conducted separately on igneous rocks, conglomerates, and sedimentary rocks. Finally this work is meant to be included in a larger effort of classification using the entire Curiosity payload.

**References:** [1] Grotzinger et al. (2013) *Science*, 10.1126/science.1242777. [2] Mangold et al. (2015) *EGU*, submitted. [3] McLennan et al. (2015) *LPS XLVI*, this issue. [4] Gasnault et al. (2013) *LPS XLIV*, Abstract #1994. [5] Gasnault et al. (2014) *Mars 8 Conf.*, Abstract #1269. [6] Schmidt et al. (2015) *LPS XLVI*, this issue. [7] Wiens R.C. et al. (2012) *Space Sci. Rev.*, 10.1007/s11214-012-9902-4. [8] Maurice S. et al. (2012) *Space Sci. Rev.*, 10.1007/s11214-012-9912-2. [9] Wiens et al. (2013) *SCAB* 82, 1-27. [10] Sautter et al. (2014) *JGR* 119, 10.1002/2013JE004472. [11] Nachon et al. (2014) *JGR* 119, 10.1002/2013JE004588. [12] Sautter et al. (2015) *LPS XLVI*, this issue. [13] Fisk et al. (2014) *AGU*, Abstract # P54B-08. [14] Le Deit et al. (2015) *LPS XLVI*, this issue. [15] Rousseeuw (1987) *J. Comput. Appl. Math.* 20, 53–65. [16] Cousin et al. (2015) *LPS XLVI*, this issue. [17] Nachon et al. (2015) *LPS XLVI*, this issue. [18] Forni et al. (2015) *LPS XLVI*, this issue.

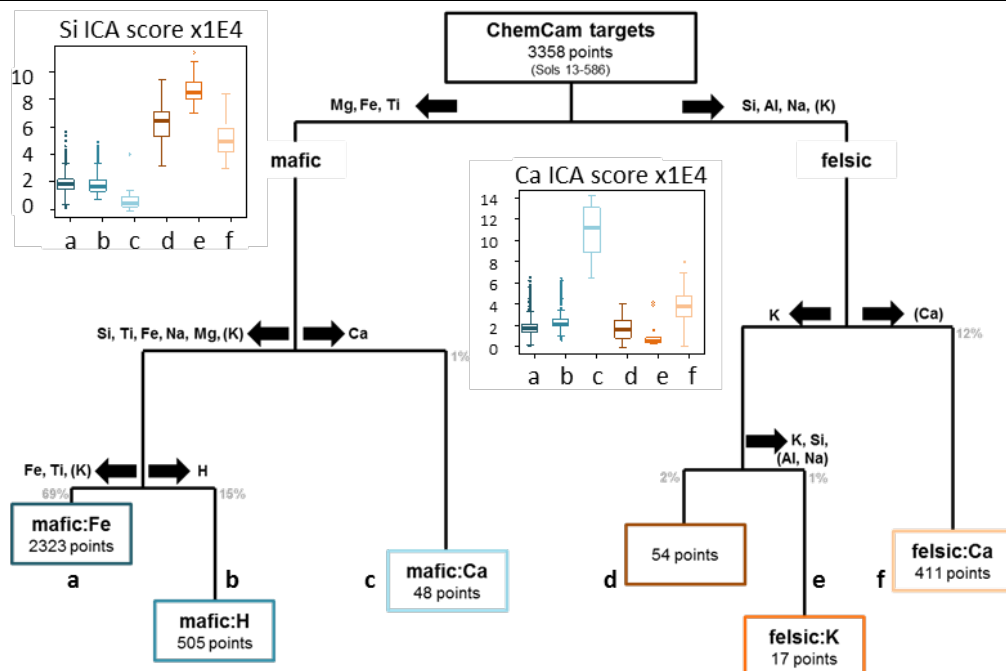


**Figure:** Schematic dendrogram for the first six groups defined with ChemCam data between Sols 13 and 586. The two insets illustrate the distribution of the ICA scores for Si and Ca in the groups.